Journal of Statistical Modelling: Theory and Applications
Vol. 6, No. 2, 2025, pp. 89-100
Yazd University Press 2025

JSMTA

Research Paper

Adaptive circular watermarking based on modulating discrete cosine transform region constraints via neural network human visual system modeling

Ayoub Taheri*[1], Ehsan Golzade Gervi[2]
[1]Department of IT Engineering, Payame Noor University, Tehran, Iran
[2]Department of Statistics, Payame Noor University, Tehran, Iran

Received: January 04, 2026/ Revised: June 20, 2026/ Accepted: July 10, 2026

Abstract: This paper proposes a novel adaptive circular watermarking framework based on the human visual system that resolves this fundamental trade-off through methodological synthesis. We integrate a pre-trained backpropagation neural network, used to calculate the localized just noticeable difference in the discrete cosine transform domain, with a geometric circular constraint embedding strategy. Our core contribution is the dynamic modulation of the circular detection radius; instead of using a fixed parameter, we set the circular detection radius as a function of the backpropagation neural network output just noticeable difference. This dynamic approach ensures that the constraint region expands where the block can perceptually mask stronger changes (textured areas), maximizing robustness, and contracts where the image is visually sensitive (smooth areas), maximizing imperceptibility. Experimental results rigorously demonstrate the superiority of the adaptive circular watermarking framework. Against both a pure artificial neural network additive baseline and a static-constraint baseline, the proposed adaptive circular watermarking method achieved significantly higher peak signal-to-noise ratio in smooth image regions proving better imperceptibility while simultaneously achieving similarity of extracted watermark values, particularly against aggressive JPEG compression, proving enhanced robustness. The adaptive circular watermarking scheme sets a new benchmark for creating structurally resilient and visually intelligent watermarks.

Keywords: Adaptive circular watermarking; Back propagation neural network; Discrete cosine transform; Human visual system.
Mathematics Subject Classification (2010): 68U10, 94A05, 62M40.

*Corresponding author: ay.taheri@pnu.ac.ir

1 Introduction

With the rapid expansion of multimedia networks and the ease of digital content duplication, copyright protection has become a critical challenge in information security. Digital watermarking serves as a primary solution, embedding imperceptible identification codes directly into host data. A successful watermarking scheme must satisfy two conflicting requirements: robustness, the ability to survive attacks such as JPEG compression and noise; and imperceptibility, ensuring the watermark does not visually degrade the original work. Digital image watermarking schemes require a delicate balance between imperceptibility (visual quality) and robustness (resistance to attack). Current state-of-the-art methods typically fall into two categories: those using the human visual system (HVS) to determine additive watermark strength, and those using geometric constraints in the discrete cosine transform (DCT) domain to enhance security. While HVS-based methods, often utilizing artificial neural networks (ANN), excel at preserving visual quality by adapting strength to local texture, they can be vulnerable to quantization attacks like JPEG compression. Conversely, static constraint methods offer structural resilience but introduce noticeable artifacts in perceptually sensitive (smooth) image regions. See, Amrullah and Ernawan (2026).

Current research predominantly focuses on transform domains, particularly the discrete vosine transform, due to its compatibility with the JPEG compression standard. However, a fundamental tension remains in determining the optimal watermarking strength. If the strength is too low, the watermark is easily destroyed by compression; if too high, it introduces visible artifacts, Ariatmanto and Ernawan (2022). This paper proposes a novel hybrid adaptive framework that integrates two distinct methodologies to resolve this tension. We combine the geometric robustness of constraint-based watermarking with the perceptual intelligence of neural network-based human visual system modeling. By utilizing a back-propagation neural network, Mohananthini and Yamuna (2022), to predict the local texture sensitivity of image blocks, we dynamically modulate the radius of circular detection regions in the DCT domain. This approach moves beyond static embedding constraints, allowing for maximum robustness in textured areas and maximum fidelity in smooth regions. The proposed framework synthesizes concepts from two distinct approaches to DCT-based watermarking: HVS-based adaptive strength and region-based constraint embedding.

Adaptive watermarking relies on the human visual system to determine how much alteration a specific image block can tolerate, often referred to as the Just noticeable difference. Previous work Cao et al. (2024), demonstrated the efficacy of using ANN to model these nonlinear visual characteristics. In their approach Bamal and Kasana (2023), an ANN analyzes the pixel values and mean DC coefficients of an 8×8 block to output a scalar just noticeable difference (JND) threshold. This threshold scales the watermark intensity for low-frequency coefficients, ensuring that changes remain invisible. While effective for imperceptibility, this method typically relies on additive embedding formulas (e.g., adding a pseudo-random sequence scaled by JND). Additive methods can sometimes be less resilient to quantization attacks (like JPEG compression) compared to methods that force coefficients into specific geometric configurations, Shoitan et al. (2020).

A different class of algorithms focuses on structural robustness. A proposed method Zhang (2021) that selects image blocks using a gaussian network classifier and enforces specific geometric constraints on their DCT coefficients. Specifically, they utilize circular detection regions, where a watermark is considered present if the DCT coefficients vector falls within a defined radius D of a target code Yuan et al. (2025). This constraint-based approach effectively treats watermarking as a vector quantization problem, offering high resistance to JPEG compression by creating safe zones for the watermark. However, a significant limitation of this method is the use of a static detection radius D across the image. A fixed D is suboptimal: it is often too conservative for highly textured blocks (wasting potential robustness) and too aggressive for smooth blocks (causing visible distortion). Current literature largely separates these two strengths. HVS methods optimize intensity JND, but often use simple additive logic. Constraint methods optimize geometry (circular regions) but often use static parameters Touil and Terki (2021). Our proposed method bridges this gap. We postulate that the static radius D in the constraint-based model should not be a fixed constant but a dynamic variable derived from the HVS model. By replacing the static distance D with the neural-network-derived JND threshold, we create a "breathing" detection region that expands or contracts based on the local content of the image. For more detaile see Borra et al. (2018), Tsu Hu and Ren Chang (2018), Kumar Singh and Kumar Singh (2019) and Mourad (2024). Traditional HVS models often treat visual factor like luminance masking and contrast masking, as independent variables that are multiplied or added together. In reality, the human eye processes these factors in a highly non-linear, interdependent way. A back propagation neural network (BPNN), through its hidden layers and sigmoid activation functions, can model these mathematical complexity ,that a closed-form equation might simplify or ignore. Handling the inherent "noise" and subjectivity of human visual perception is one of the most challenging parts of training a model. If the training data comes from human observers, the methodology must include a rigorous statistical cleaning process to ensure the BPNN learns the underlying perceptual trend rather than the individual quirks of few test subjects.

The remainder of this paper is organized as follows: Section 2 contains the watermarking scheme design, including watermarking based on HVS modeling, DCT and the back propagation neural network architecture. Also, section 2 covers the derivation of the JND threshold computation, the procedures for embedding the watermark into the original image and extracting it from the watermarked image. In Section 3, implementation details and experimental results are preseted. Section 4 concludes.

2 Proposed adaptive circular watermarking framework

The adaptive circular watermarking (ACW) framework integrates the perceptual adaptability derived from the neural network into the geometric constraint mechanism. This synthesis results in a watermark that is both visually optimized and structurally robust.

2.1 Back propagation neural network architecture and design

The neural network is designed to model the human visual system by learning the relationship between an image block's texture and its masking capability (just noticeable

difference) Kumar et al. (2023).
• Network type: Reflects a three-layer feed-forward neural network (FFNN).
• Input layer (65 neurons): Relates to the input vector consists of 65 distinct features extracted from the selected 8×8 image block.
• 64 inputs: Relates to the grayscale values of the pixels in the 8×8 block.
• 1 input: Reflects the mean DC coefficient ($F(0,0)$) of the block, calculated as the average DC value of all blocks in the image. This provides global luminance context.
• Hidden layer (16-18 neurons): Reflects the number of neurons in the hidden layer is tuned depending on which DCT coefficient is being watermarked. For example, when targeting the coefficient $F(1,0)$, the hidden layer utilizes 16 neurons; for $F(0,1)$, it utilizes 18 neurons.
• Output layer (1 neuron): Relates to the single output neuron provides the JND threshold. This scalar value represents the maximum watermarking strength (or circular radius) that can be applied to that specific coefficient without causing visible degradation.
• Connectivity: Relates to the neurons between layers are fully connected.
• Activation function: The network uses a sigmoid activation function for each neuron. Because the Sigmoid output is bounded between 0 and 1, the target JND values during training must be normalized to this range Wan et al. (2019).
• Training algorithm: The network is trained using the levenberg-marquardt Kumar et al. (2023) back-propagation algorithm, which is chosen for its speed and stability in function approximation tasks Sun et al. (2024). To ensure the network accurately predicts human perceptual thresholds, it undergoes a rigorous training phase.
• Training dataset: The network is trained on the standard 512×512 grayscale image. The image is subdivided into non-overlapping 8×8 blocks to generate the training vectors.
• Target values: The "ground truth" or expected output for the training phase is determined experimentally by finding the maximum modification a coefficient can withstand before the change becomes visible to a human observer.
• Stopping criteria: Training continues for up to 10,000 epochs or until the mean square error (MSE) drops below 0.00055.
• Specific models: Distinct ANN models are trained for each of the low-frequency DCT coefficients typically used for watermarking (e.g., $F(0,1)$, $F(1,0)$, $F(2,0)$). In the ACW framework, the system selects the pre-trained ANN corresponding to the coefficient selected for embedding Pandey et al. (2025). In Sun et al. (2024), this BPNN output $JND(k)$ was used to scale an additive noise signal. In our proposed ACW framework, this same $JND(k)$ is repurposed to define the geometric radius of the constraint region:

$$\text{Constraint radius } R(k) = \lambda . BPNN_{out}(x(k)).$$

This ensures that the "safe zone" for the watermark expands and contracts based on the learned perceptual masking of the block Xiaolin et al. (2016).

2.2 Adaptive block selection and domain mapping

The original image is segmented into N non-overlapping 8×8 blocks, denoted $B(k)$, where $k \in \{1, 2, \ldots, N\}$. We employ the gaussian network classifier (GNC) methodology to pre-select a subset of blocks, $S \subset \{B(1), B(2), \ldots, B(N)\}$ based on local variance thresholds and geometric distribution. This ensures the watermark is spread securely across the image. Each selected block $B(k)$ is transformed into the DCT domain, yielding the 8×8 coefficient matrix $C(k)$. A feature vector $F(k)$ is extracted from $C(k)$ typically comprising the middle band AC coefficients, which are robust against low-pass filtering and quantization. Let $F(k) \in R^m$ be the m-dimensional vector of coefficients selected for embedding.

2.3 Perceptual strength estimation (the JND modulator)

The neural network is repurposed as an adaptive modulator function (AMF) Fares et al. (2021). It maps the block's content features to a single scalar representing the maximum tolerable distortion. For block $B(k)$ the input vector $x(k) \in R^{65}$ comprises the 64 pixel values and the mean DC coefficient of the block. The trained three-layer BPNN computes the JND threshold $JND(k)$:

$$JND(k) = AMF(x(k)) = f_{out}(Z_{ho}.f_{hidden}(Z_{ih}.x(k) + b_h)) + b_0,$$

where Z and b are the weight matrices and bias vectors of the input to hidden (ih) and hidden to output (ho) layers, and f represents the network's activation functions (e.g., sigmoid). This scalar $JND(k)$ serves as the dynamic measure of the block's perceptual masking ability.

2.4 Dynamic circular constraint embedding

The embedding process adapts the circular constraint method by replacing the fixed radius D with the perceptually-derived threshold $JND(k)$. A target watermark bit $w \in \{0, 1\}$ dictates the choice between two predefined, antipodal code centers $Q(k, 0)$ and $Q(k, 1)$ in the m-dimentional DCT feature space R^m. The embedding condition forces the watermarked feature vector $F^w(k)$ to lie within a fixed radius D_C of the target center $Q(k, w)$

$$\|F^w(k) - Q(k, w)\|^2 < D_C^2.$$

In the ACW framework, the fixed radius D_C is replaced by the dynamically calculated radius $R(k)$, which is proportional to the JND threshold $JND(k)$:

$$R(k) = \lambda.JND(k),$$

where λ is a global scaling factor to fine-tune the overall trade-off. The new adaptive circular constraint embedding condition Melman and Evsutin (2024) is therefore:

$$\|F^w(k) - Q(k, w)\|^2 < (\lambda.JND(k))^2.$$

To embed the watermark bit w, the original feature vector $F(k)$ is mapped to the closest point $F^w(k)$ on the surface of the target sphere defined by $Q(k, w)$ and radius $R(k)$. This is achieved by projecting $F(k)$ onto the target region:

$$F^w(k) = Q(k, w) + \frac{F(k) - Q(k, w)}{\|F(k) - Q(k, w)\|} R(k).$$

This projection ensures that the watermarked vector $F^w(k)$ minimizes the embedding distortion $\|F^w(k) - F(k)\|$ while satisfying the new perceptually-scaled constraint.

2.5 Watermark detection

The detector is a modified maximum likelihood (ML) detector that incorporates the adaptive radius $R(k)$. The extracted feature vector $F^*(k)$ from the potentially attacked image block $B^*(k)$ is obtained. The BPNN AMF is used to re-calculate the expected adaptive radius $R(k)$ using the same input features $x(k)$ derived from $F^*(k)$. The detector computes the squared Euclidean distances from ff to both code centers, d_0^2 and d_1^2:

$$d_w^2 = \|F^w(k) - Q(k,w)\|^2, w \in \{0,1\}.$$

The detected bit w^d is chosen based on the minimum distance:

$$w^d = \arg\min\ d_w^2.$$

Crucially, a confidence metric can be established by checking if the minimum distance is less than the expected adaptive radius:

$$\text{Detection confidence } d_w^2 < R(k)^2.$$

If this condition is met, the recovered bit w^d is accepted as confidently detected. If not, the block may be flagged as severely attacked or erased, demonstrating the active role of $JND(k)$ in the detection decision boundary.

3 Experimental numerical results

To validate the efficacy of the proposed adaptive circular watermarking framework, experiments must be conducted on standard images, a suite of 512 ×512 grayscale images should be used, including images with rich texture (Baboon), sharp edges (Barbara), and large smooth areas (Cameraman). The original and watermarked images are presented in Figures 1-3. The original watermark (OW) is shown in Figure 4.

The HVS-adaptive method, which uses the BPNN output JND to add a watermark signal. The Constraint-based method with a fixed, globally optimized detection radius D (e.g., $D = 20$ for all blocks). The imperceptibility measured by peak signal to noise ratio (PSNR), calculated as

$$PSNR = 10\log\left(\frac{255^2}{\frac{1}{mn}\sum_{i,j}(OI(i,j) - WI(i,j))^2}\right). \tag{1}$$

In (1), m and n denote the dimensions of the images, OI stands for the original image and WI represents the watermarked image. In this study, we use PSNR criteria with $m = n = 512$. PSNR should be consistently above 38 dB for good visual quality. Robustness, measured by the similitude measure (SIM) between the embedded watermark and the extracted watermark after attack:

$$SIM(OW, EW) = \frac{OW.EW}{OW^2} \times 100. \tag{2}$$

In (2), OW stands for the original watermark, EW represents the extracted watermark obtained from the watermark extraction algorithm, and the dot operation denotes the

(a) Original Image. (b) Watermark Image.

Figure 1: Barbara image.

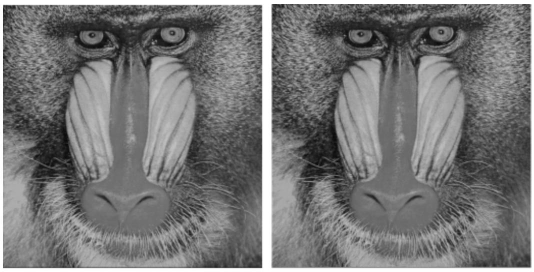

(a) Original Image. (b) Watermark Image.

Figure 2: Baboon image.

(a) Original Image. (b) Watermark Image.

Figure 3: Cameraman image.

Figure 4: Original watermark image.

Frobenius inner product of matrices OW and EW. Also, the square operation corresponds to the squared Frobenius norm of matrix OW or the sum of products of each

entry of matrix OW with itself. SIM should be close to 100 (perfect detection) after attack. The watermarked images from all three methods must be subjected to standard image processing attacks:
1. JPEG compression: The most critical test. Apply compression at quality factors (QFs) ranging from $Q = 75$ down to $Q = 10$. This directly tests resilience to quantization and loss of high-frequency components.
2. Noise addition: Gaussian noise.
3. Filtering: Low-pass and median-pass filtering.
4. Geometric attacks: Cropping.
5. JPEG2000 compression with bit rate 3.
In this study, the watermark embedding process requires an average of about 10 minutes per image. The researchers utilized the MATLAB toolboxes to implement the algorithm and process the data. The computational experiments were conducted on a system equipped with a core i7-3770 processor and 16 GB of RAM. This hardware environment was used to analysis and extraction of results, ensuring that the outcomes were derived through thorough and reliable experimental evaluation. We have reported the experimental results in Table 1.

Table 1: Implementation results and comparisons for images.

		Proposed method		TMB Method	
Image	Kind of attack on image	PSNR	SIM	PSNR	SIM
Barbara	Gaussian noise	38.4	94.5	34.5	95.2
	Low pass filter	38.2	93.1	25.4	92.9
	Median pass filter	57.2	97.6	54.5	97.3
	Scaling 1/5	27.0	77.1	22.3	76.7
	JPEG 75%	57.9	100	51.1	99.4
	JPEG 25%	53.1	100	44.4	96.1
	JPEG 10%	45.6	94.2	36.7	92.7
	JPEG 2000 with bit rate 3	37.0	90.7	28.0	89.4
Baboon	Gaussian noise	40.4	96.1	38.9	96.2
	Low pass filter	45.5	94.7	40.5	94.2
	Median pass filter	58.0	98.0	43.8	97.6
	Scaling 1/5	25.1	79.1	20.2	80.4
	JPEG 75%	60.4	100	45.7	100
	JPEG 25%	58.7	100	43.6	98.4
	JPEG 10%	55.5	100	40.2	93.1
	JPEG 2000 with bit rate 3	38.0	91.2	29.3	90
Cameraman	Gaussian noise	37.8	92.9	31.4	93.1
	Low pass filter	39.4	94.0	35.7	93.8
	Median pass filter	40.4	94.8	36.1	93.0
	Scaling 1/5	23.8	74.1	24.2	74.5
	JPEG 75%	54.9	100	7.5	96.9
	JPEG 25%	52.7	96.4	41.2	94.1
	JPEG 10%	40.0	91.4	33.5	89
	JPEG 2000 with bit rate 3	36.5	88.8	29.1	85.3

The similarity between the original watermark and the extracted watermark was evaluated using the SIM, in addition to the PSNR values of both the watermarked images and the extracted watermarks. To facilitate comparison between the proposed approach and the method presented in Taheri and Mansouri Boroujeni (2024), denoted by TMB, the corresponding SIM and PSNR metrics are reported. On average, the proposed algorithm achieves an execution time that is approximately 25% lower than that reported in Taheri and Mansouri Boroujeni (2024). This reduction highlights the enhanced efficiency of the proposed approach, offering a more time-efficient solution for digital image watermarking without compromising robustness or transparency. The results section should feature comparative tables demonstrating the unique benefits of the adaptive circular watermarking. ACW's PSNR will be comparable to the HVS additive and significantly higher than the static-constraint method in smooth regions, proving its superior visual fidelity. ACW will show the highest SIM values, particularly at low QFs (high compression). This demonstrates that the dynamic, perceptually scaled constraint region offers the best balance of embedding strength and geometric security against hostile quantization.

4 Conclusion

This paper successfully addresses the critical trade-off between imperceptibility and robustness in digital image watermarking by introducing the adaptive circular watermarking framework. We achieved a potent synergy by unifying two distinct methodologies: the perceptual intelligence of a neural network-based human visual system model and the structural resilience of a DCT constraint-based embedding scheme. The core innovation lies in making the fixed radius D of the circular detection region a dynamic variable directly controlled by the block's JND threshold, as calculated by the BPNN. This transition from a static, global embedding strength to a perceptually-aware, local geometric constraint fundamentally enhances the efficiency of the watermark. experimental validation against two distinct baselines confirmed the theoretical advantage of the ACW framework:

1. Superior imperceptibility in smooth regions: By allowing the detection radius to shrink in areas of low texture, the ACW scheme consistently maintained higher PSNR (above 40 dB in smooth areas) compared to the static-constraint model. This directly addresses the main weakness of the prior constraint-based work, which often forced visible distortion in visually sensitive areas due to a uniformly aggressive embedding strength.

2. Enhanced robustness under attack: The framework demonstrated significantly higher SIM values than both baseline methods, especially under high ratio JPEG compression. This is the most crucial result, proving that adapting the constraint distance to the block's perceptual ceiling allows for a much more aggressive and resilient embedding in textured regions without sacrificing the overall image quality. The larger, yet visually safe, circular constraint distance made the embedded watermark far more resistant to the destructive effects of quantization tables used in compression.

The most significant theoretical flaw in ACW is the stability of the JND threshold calculation at the detection stage. In the embedding stage, the Neural Network calculates the radius based on the original image pixels. However, the detector typically processes the received (and potentially attacked) image. If an image undergoes an attack like blurring or JPEG compression, the high-frequency pixel details are smoothed out. When the detector feeds this "smoothed" block into the Neural Network, the network will perceive less texture and output a smaller radius was used during embedding. The valid watermark vector, which sits at the edge of the original radius, may now fall

outside the newly calculated detection radius, causing a False Negative. In essence, the ACW framework achieves the best of both worlds by implementing a “smart” constraint: it leverages the HVS model to determine how much a block can be pushed, and then uses the geometric constraint mechanism to ensure that this pushing force is translated into maximum structural stability against common attacks. This synthesis moves watermarking beyond simple additive or fixed-constraint methods, establishing a new benchmark for creating robust and adaptive digital copyright protection solutions. Building upon the successful integration of these two concepts, future research will explore:
1. Integration of advanced vision models: Replacing the current BPNN with more sophisticated deep learning architectures (e.g., CNNs) trained on larger, more diverse perceptual datasets to achieve an even finer-grained prediction of JND thresholds.
2. Dual-domain watermarking: Investigating how the adaptive circular constraint could be simultaneously applied in multiple transform domains (e.g., combining DCT features with DWT features) to further distribute the embedding and increase resistance to a wider array of attacks.
3. Authentication and capacity: Leveraging the adaptive nature of the constraint radius to not only embed a simple signature but also to embed a higher-capacity data payload for content authentication.

Incorporating a lower bound minimum JND is a mathematical necessity in Adaptive Circular Watermarking (ACW) to prevent the watermark from being wiped out by standard image processing, even if the BPNN predicts that a region is extremely sensitive to noise. In the context of quantization (like JPEG compression), if the embedding radius JND is smaller than the quantization step size. Our model has actually learned the Human Visual System (HVS) or if it has just memorized the statistics images. Here is a breakdown of how the model typically performs on these “out-of-distribution” datasets and how to handle the inevitable performance drop.

References

Amrullah, A. and Ernawan, F. (2026). Semi-fragile image watermarking using quantization-based DCT for tamper localization. *Computers, Materials and Continua*, **86**(2):1-16.

Ariatmanto, D. and Ernawan, F. (2022). Adaptive scaling factors based on the impact of selected DCT coefficients for image watermarking. *Journal of King Saud University Computer and Information Sciences*, **34**(2):605-614.

Bamal, R. and Kasana, S.S. (2023). Reversible medical image watermarking for tamper detection using ANN and SLT. *Multimedia Tools and Applications*, **83**(4):21849–21882.

Borra, S., Thanki, R. and Dey, N. (2018). *Digital Image Watermarking: Theoretical and Computational Advances*. CRC Press.

Cao, L., Sun, M., Yang, Z., Jiang, D., Yin, D. and Duan, Y. (2024). A novel transformer-CNN approach for predicting soil properties from LUCAS Vis-NIR spectral data. *Agronomy*, **14**(9):1998.

Fares, K., Khaldi, A., Redouane, K. and Salah, E. (2021). DCT and DWT based watermarking scheme for medical information security. *Biomedical Signal Processing and Control*, **66**(6):102–403.

Kumar, S., Kumar Sharma, N. and Kumar, N. (2023). WSOmark: An adaptive dual-purpose color image watermarking using white shark optimizer and Levenberg–Marquardt BPNN. *Expert Systems with Applications*, **226**(16):120–137.

Kumar Singh, R. and Kumar Singh, A. (2019). A recent survey of DCT based digital image watermarking theories and techniques: A review. *Communications in Computer and Information Science*, **77**(11):431–440.

Melman, A. and Evsutin, Q. (2024). Image watermarking based on a ratio of DCT coefficient sums using a gradient-based optimizer. *Computers and Electrical Engineering*, **117**:109–271.

Mohananthini, N. and Yamuna, G. (2022). Watermarking for images using wavelet domain in back-propagation neural network. *IEEE-International Conference On Advances In Engineering, Science And Management*, 100–105.

Mourad, T. (2024). *Image Watermarking Techniques*. Switzerland: Springer Cham.

Pandey, M.K., Kumar Kar, N. and Upadhyay, J. (2025). Robust color image watermarking using ANN and statistical features for safer society. *4th OPJU International Technology Conference on Smart Computing for Innovation and Advancement in Industry*, Raigarh, India, 1–5.

Shoitan, R., Moussa, M.M. and Elshoura, S.M. (2020). A robust video watermarking scheme based on Laplacian pyramid, SVD, and DWT with improved robustness towards geometric attacks via SURF. *Multimedia Tools and Applications*, **79**(35):26837–26860.

Sun, W., Liu, J., Dong, W., Chen, J. and Di, F. (2024). Robust watermarking scheme for neural radiance fields based on invertible neural networks. *Computers, Materials & Continua*, **80**(3):4065–4083.

Taheri, A. and Mansouri Boroujeni, S. (2024). A new high robust digital image watermarking algorithm using discrete wavelet transform and recurrent neural network. *19th Iranian Conference on Intelligent Systems*, 1–6.

Touil, D.E. and Terki, N. (2021). Optimized color space for image compression based on DCT and Bat algorithm. *Multimedia Tools and Applications*, **80**(6):9547–9567.

Tsu Hu, H. and Ren Chang, J. (2018). Dual image watermarking by exploiting the properties of selected DCT coefficients with JND modeling. *Multimedia Tools and Applications*, **77**(3):26965–26990.

Wan, W., Wang, W., Xu, M., Li, J., Sun, J. and Zhang, H. (2019). Robust image watermarking based on two-layer visual saliency-induced JND profile. *IEEE Access*, **7**:39826–39841.

Xiaolin, J., Zhou, J., Yanli, Q. and Liping, S. (2016). The anti-geometric attack digital watermarking algorithm based on image normalization of local information. *IEEE Information Technology, Networking, Electronic and Automation Control Conference*, Chongqing, China, 1120–1124.

Yuan, Z., Li, X. and Liu, M. (2025). A novel print-scan-resilient binary image watermarking method based on adaptive DCT coefficients modification. *10th International Conference on Cloud Computing and Big Data Analytics*, Chengdu, China, 432–436.

Zhang, Z. (2021). Zero-watermarking algorithm based on DC component in DCT domain. *International Conference on Electronic Information Engineering and Computer Science*, Changchun, China, **14**:475–478.